CHAPTER 8
VIBRO TECHNIQUES FOR GROUND IMPROVEMENT

8.1. General

Ground improvement techniques using vibratory systems are applicable mostly in areas loaded by restricted amount of pressure, i.e. highway and railway fill embankments, airport, tank etc., in order to satisfy the general stability, decrease the amount of total and differential consolidation settlement, control the time of consolidation. In addition, those systems are used to prevent/improve the slope stability and mitigate the sites under risk of liqufiaction potential.

Although the methodology and the equipments are similar, ground improvement techniques using vibratory sytems are classified under two main topics (Figure 8.1):

(i) Cohesionless Soils (Sand): Vibro-Compaction
(ii) Cohesive Soils (Clay): Vibro-Replacement (Stone Columns)

Improvement mechanism and the design criteria are exactly different from each other.

In vibro-compaction method:
- Crushed stone is filled into the borehole and compacted.
- Soil deposit is completely improved.
- Improved soil has significiantly higher density and shear strength and lower compactibility with respect to original (before improvemet) soil.

In vibro-replacement method:
- Crushed stone is filled into the borehole and compacted.
- Soil deposit is partially improved (only at the application locations, there is no significant improvement between the application locations).
- Consequently, soil (soft) – stone column (rigid) composite matrix is developed.

To sum up, by using vibratory systems; in cohesionless soils overall deep compaction and in cohesive soils composite soil with rigid columns are satisfied. By using vibrotory systems, ground is improved by owing to:

(i)   Increase in bearing capacity and shear strength
(ii)   Decrease in compactibility and compressibility, decrease in time of consolidation
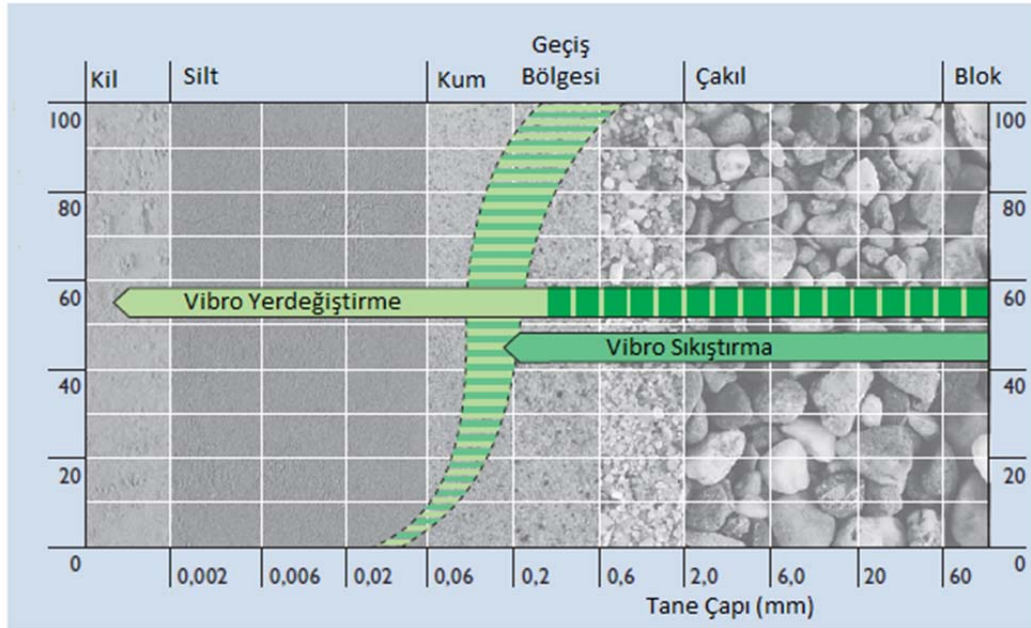(iii)   Prevent the risks of liquefaction and lateral dispersibility

Figure 8.1. Gradation ranges for the application of vibro-compaction and vibro-replacement methods (Barksdale et al., 1983)

8.2. Vibrators

In application of vibratory system, electrically or hydraulically actuated vibrators located near the bottom of the probe are used. These vibrators are also called as *Vibroflot.* Motor of the vibroflot rotates the eccentric mass, satisfies vibration and force in lateral direction thus; by water/air jet vibroflot can penetrate into the soil (Figures 8.2, 8.3 and 8.4).
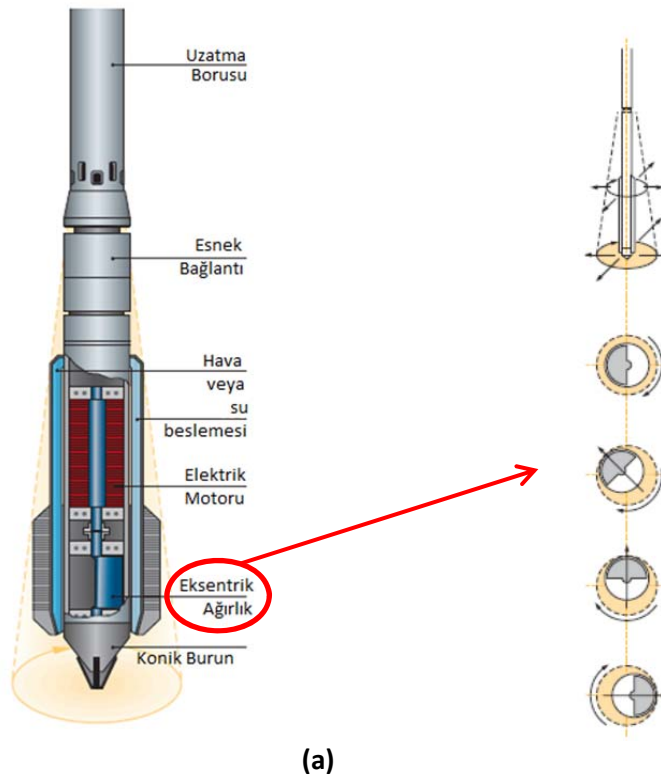

(a)   (b)

Figure 8.2. (a) Vibroflot and (b) rotation of eccentric mass (Barksdale et al., 1983)

Nozzles for water jet

Figure 8.3. Typical vibroflot

Figure 8.4. Penetration of vibroflots

8.3. Construction Methods

i. Wet Top Feed Method (in vibro-replacement method) →Figure 8.5
   ➢ Water/air jet is used
   ➢ For sands and silty sands under ground water level
ii. Dry Top Feed Method (in vibro-displacement method)
   ➢ Same with the wet method but dry (no water jet)
   ➢ For soft but stable cohesive soils (c_u > 30 kN/m^2)
iii. Dry Bottom Feed Method (in vibro-displacement method) →Figure 8.6
   ➢ For unstable (collapsible) clayey and silty soils (c_u < 30 kN/m^2)
iv. Sand Compaction Piles (in vibro-composer method) →Figure 8.7
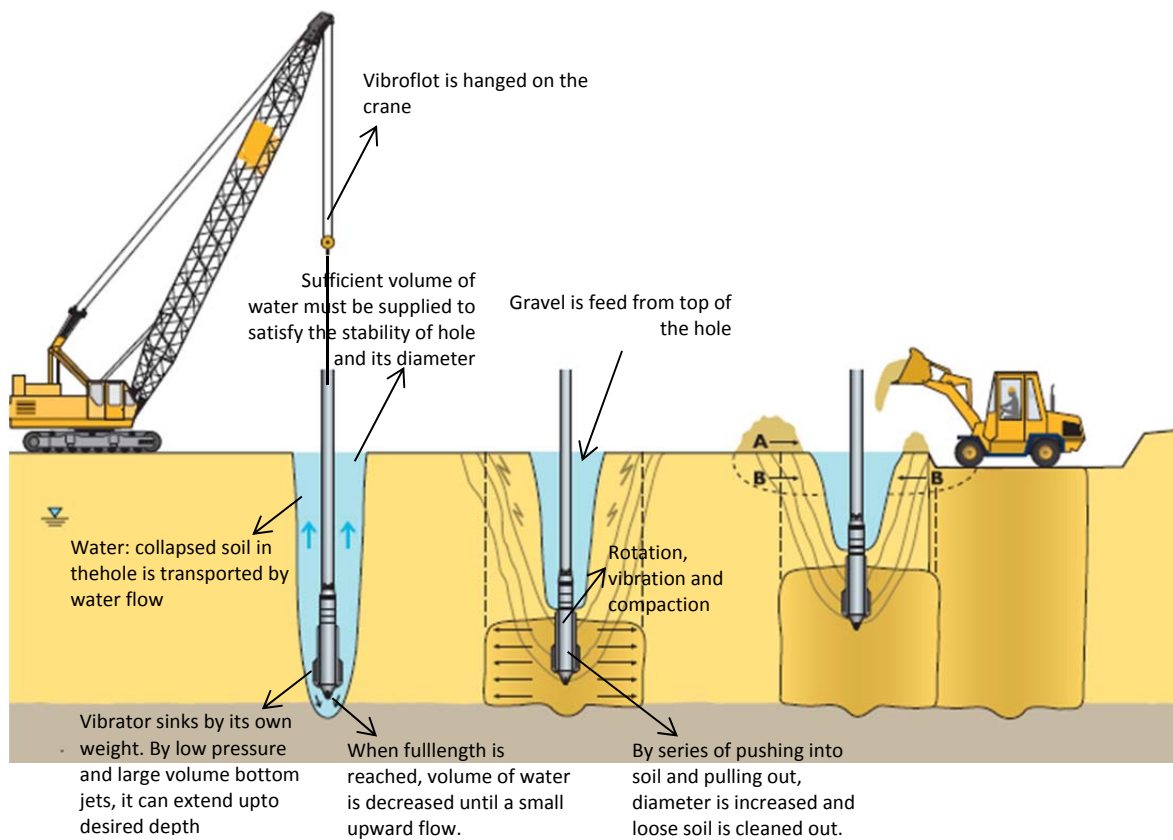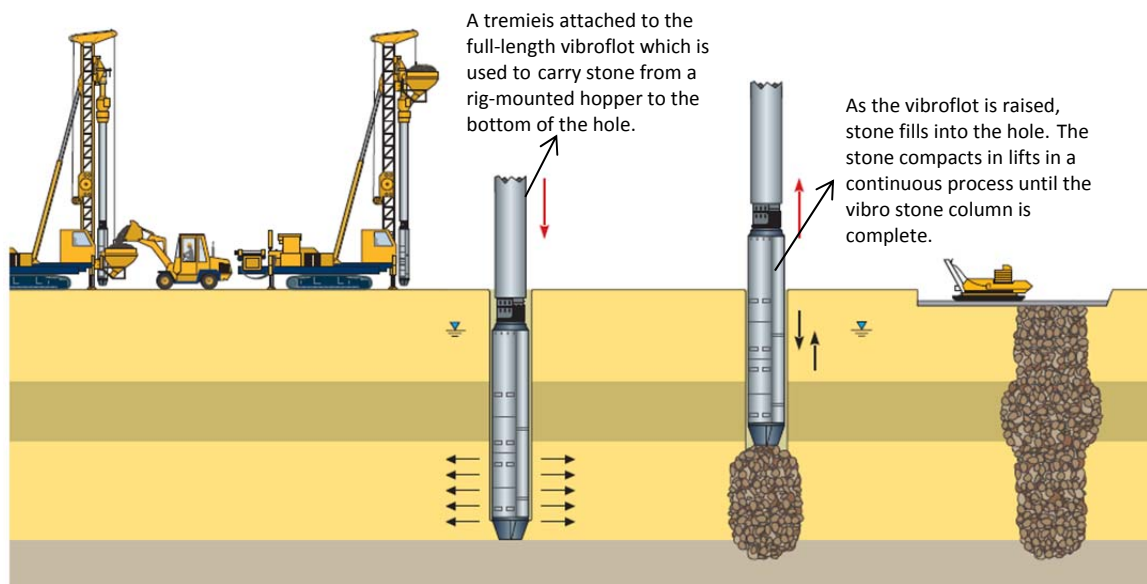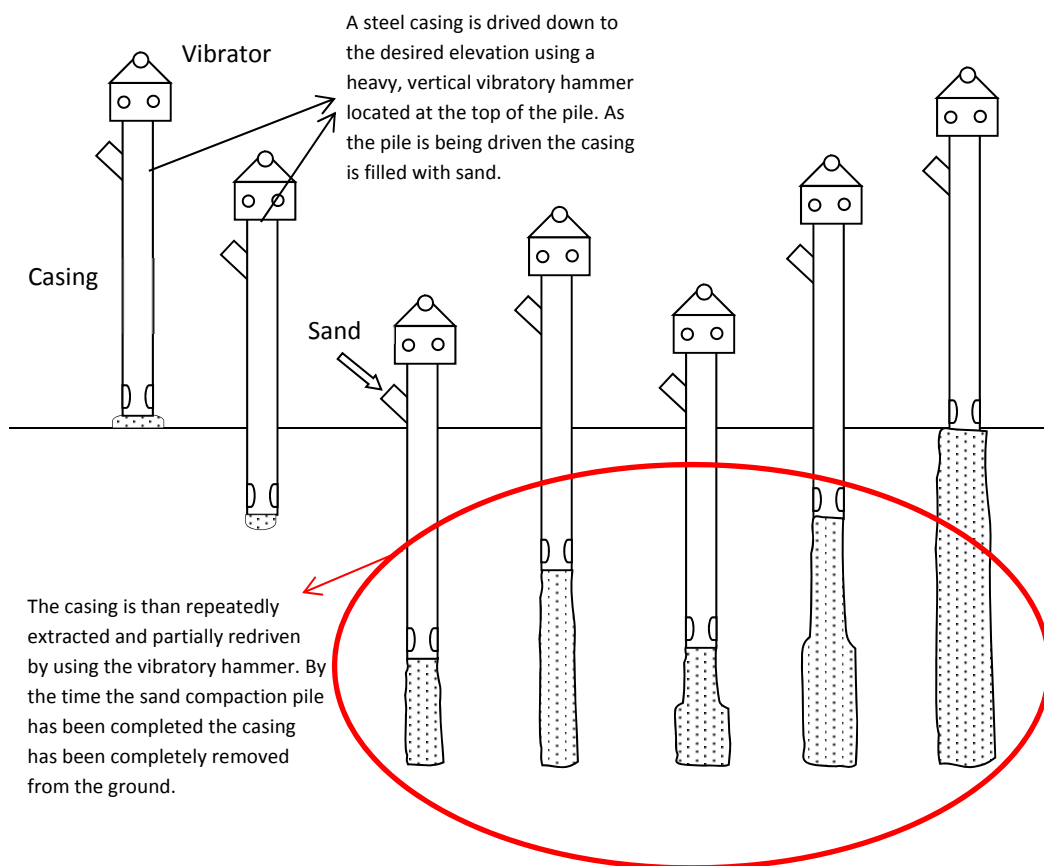v. Impact/Compacted Granular Piers (Geopier^{TM})→Figure 8.8

Vibroflot is hanged on the crane

Sufficient volume of water must be supplied to satisfy the stability of hole and its diameter

Gravel is feed from top of the hole

Water: collapsed soil in thehole is transported by water flow

Rotation, vibration and compaction

Vibrator sinks by its own weight. By low pressure and large volume bottom jets, it can extend upto desired depth

When fulllength is reached, volume of water is decreased until a small upward flow.

By series of pushing into soil and pulling out, diameter is increased and loose soil is cleaned out.

Figure 8.5. Wet top feed method

A tremieis attached to the full-length vibroflot which is used to carry stone from a rig-mounted hopper to the bottom of the hole.

As the vibroflot is raised, stone fills into the hole. The stone compacts in lifts in a continuous process until the vibro stone column is complete.

Figure 8.6. Dry bottom feed method

Vibrator

A steel casing is drived down to the desired elevation using a heavy, vertical vibratory hammer located at the top of the pile. As the pile is being driven the casing is filled with sand.

Casing

Sand

The casing is than repeatedly extracted and partially redriven by using the vibratory hammer. By the time the sand compaction pile has been completed the casing has been completely removed from the ground.

Figure 8.7. Sand compaction piles

5
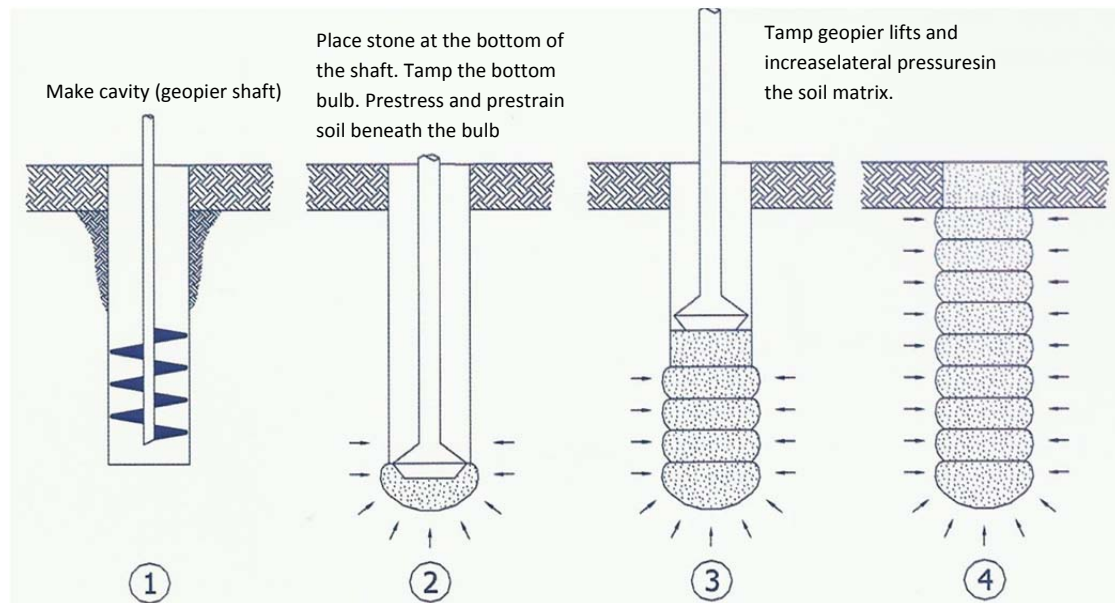
(a)
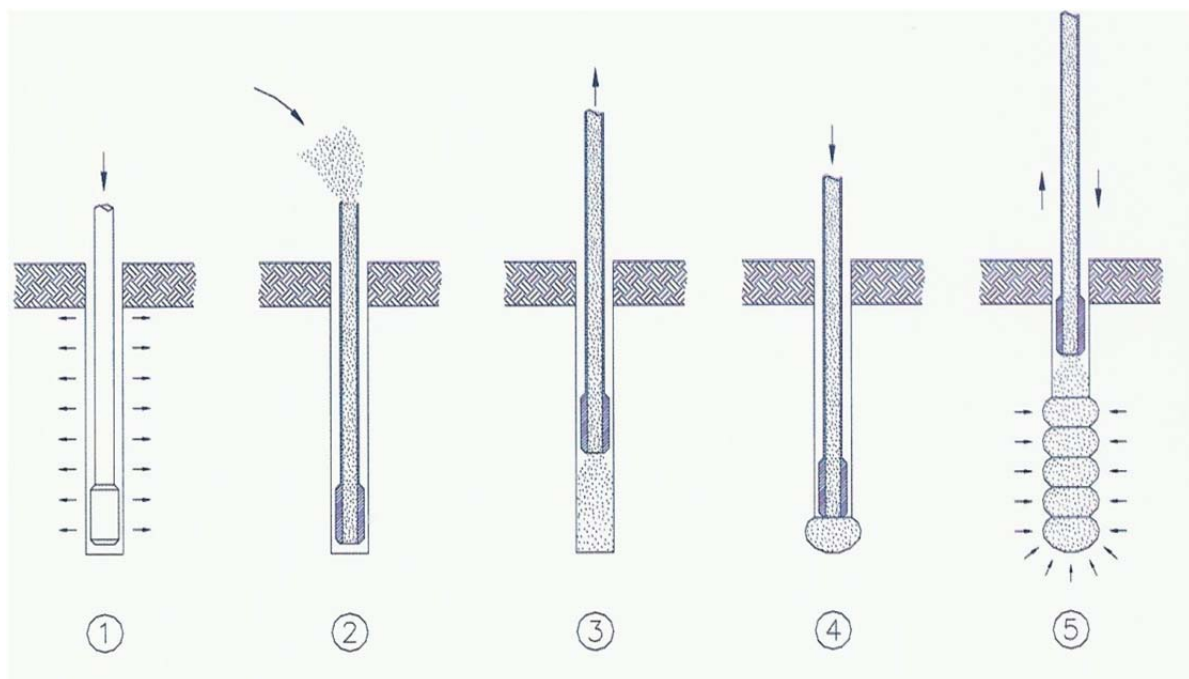
(b)

Figure 8.8. (a) Compacted and (b) impact granular piers

8.4. Vibro-Compaction Method

8.4.1. Application Principles

By the effect of vibration and centrifugal force, density of natural soil surrounding the drillhole increases, compacts and volume decreases (Figure 8.9). The volume loss due to compaction is balanced by the crushed stone. At the end of the vibro-compaction, densified sand column is developed around the vibrator. The column is composed of high density core and volume with gradually decreasing density in the radial direction. Diameter of the column varies within 3 m to 6 m depending on the gradation of the original soil and the properties of vibrosystem. In general, vibro-compaction is used to improve cohesionless soils with fine content (FC) smaller than 15%, relative density (D_r) lower than 50% and standard penetration blow count (SPT-N) smaller than 20 blows / 30 cm.
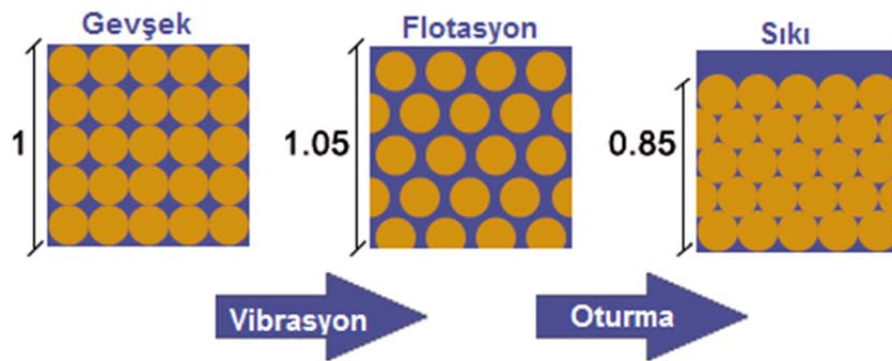

Figure 8.9. Mechanism of improvement in vibro-compaction method

Various vibrosystems are used in vibro-compaction applications. One of the most common vibrosystem is vibrocomposer satisfying high density sand columns by both radial and vertical vibration (*sand compaction pile method*). This system is composed of a heavy vibrator attached on the steel pipe and a hole in the pipe in order to feed sand. At specified depths, system is pushed up and down to densify the sand at the bottom of the hole and diameter of column is increased by the lateral translational motion.

8.4.2. Design

Disposition Patterns:

Sand compaction piles are generally constructe in square/rectangular or triangular patterns (Figure 8.10). The replacement ratios (a_s) for different arrangements are represented as:

$$a_s = \frac{A_s}{A} = \frac{A_s}{X^2} \; or \; \frac{A_s}{X_1 X_2} \quad (for \; square \; or \; rectangular \; pattern)$$

$$a_s = \frac{A_s}{A} = \frac{2}{\sqrt{3}}\frac{A_s}{X^2} \qquad (for\ triangular\ pattern)$$

Where; A_s: cross-section area of sand pile, A: area of original ground improved by single sand pile (tributary area), X_1, X_2 and X: pile space.

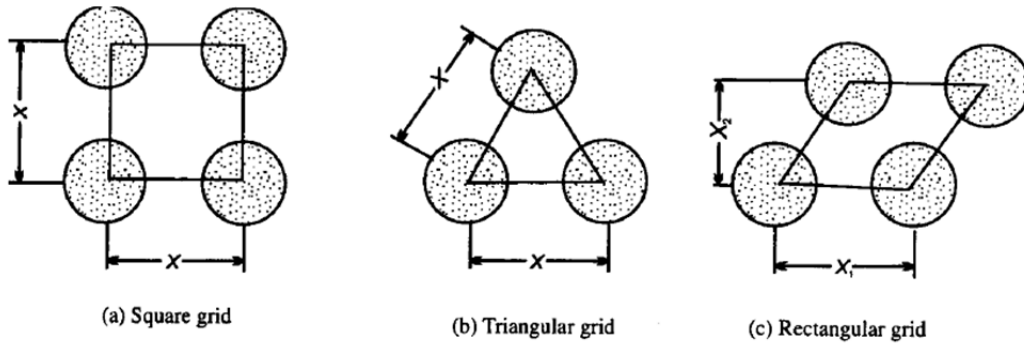
(a) Square grid   (b) Triangular grid   (c) Rectangular grid

Figure 8.10. Arrangements of sand compaction piles

Design Principle:

Figure 8.11 shows the principles of soil improvement by the sand compaction pile method. Sand amounting to Δe is introduced into the original ground, the volume which is represented by $(1+e_0)$. By the compaction the original void ratio (e_0) can be reduced to void ratio after ground improvement (e_1).

(Original ground)   (After improvement)
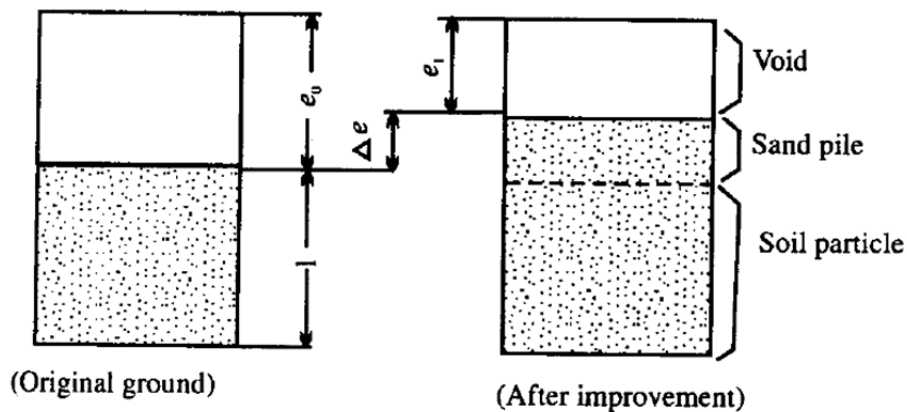
Figure 8.11. Principle of soil improvement by sand compaction pile method
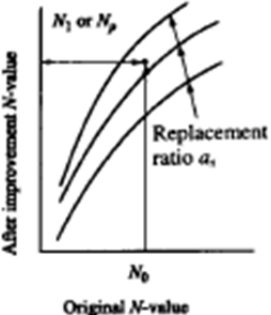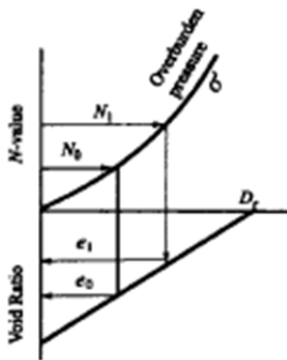
The replacement ratio (a_s) can be represented as:

$$a_s = \Delta e/(1 + e_0) = (e_0 - e_1)/(1 + e_0)$$

Design Procedure:

Three different approaches are normally employed in the design of sand compaction pile projects as shown in Table 8.1. Evaluation of the relationship between SPT-N value and void ratio is the key for selecting the proper design approach.

Table 8.1. Design approaches of sand compaction piles

Setting the N-value of Original Ground (No)
obtained from investigation results and target N value(N_1)

Method A	Method B	Method C
Step–1 (1) In case when the target N-value is evaluated by the N-value between piles (N_1), required replacement ratio obtained from Fig. 5.12(a). (2) In case when the target N-value is evaluated as $N = (1-a_s)N_1 + a_s \cdot N_p$ as can be obtained from Figs. 5.12(a) and (b) by trial and error. *Step–2* Pile spacing x can be determined from a_s obtained from *step–1*	*Step–1* e_{max} and e_{min} can be found from Fig. 5.14(a) using grain size distribution of original ground (D_{60} or D_p). D_p represents particle size with maximum frequency. *Step–2* Relationship between D_r and e can be found in Fig. 5.14(c) from e_{max} and e_{min} obtained in *step–1*. *Step–3* $\Delta e = (e_0 - e_1)$ is selected using Fig. 5.14(b) and (c). a_s then can be determined from Eq. (5.3) *Step–4* Pile spacing x can be determined from a_s obtained from *step–3*.	*Step–1* e_{max} and e_{min} can be found from fines content (F_c) using following equation. $e_{max} = 0.02F_c + 1.0$ $e_{min} = 0.008F_c + 0.6$ *Step–2* Relative density D_{r0} and e_0 can be obtained from N_0 (N-value of original ground) and constraints σ'_v (kgf/cm²) using following equation $D_{r0} = 21\sqrt{N_0/(0.7+\sigma'_v)}$ $e_0 = e_{max} - \dfrac{D_{r0}}{100}(e_{max} - e_{min})$ *Step–3* Reduction factor β to target N-value is determined from fines content as follows $\beta = 1.05 - 0.51 \log F_c$ *Step–4* Target N-value N'_1 is determined taking reduction factor β into account $N'_1 = N_0 + (N_1 - N_0)/\beta$ *Step–5* e_1 is selected from the equation shown in *step–2* providing that N_0 should read as N'_1. *Step–6* a_s is finally decided from e_0 and e_1 using Eq. (5.3) *Step–7* Pile spacing x can be decided from a_s obtained in *step–6*
 Schematic figure showing the method to handle Fig. 5.12 and 5.14		

1. Method A (conventional chart established by site data)

Conventional charts established by previous work records are used in this method (Figure 8.12). Conventional charts include the relationship between SPT-N values of the original ground and SPT-N measured between piles or at the center of a sand pile after improvement. The replacement ratio (a_s) is designed from the SPT-N value of the original ground and the target SPT-N value after improvement. The evaluation of improvement is normally made using the average of the SPT-N values measured between piles rather than SPT-N values measured at the center of the pile. The design charts in the Figure 8.12 can be applied only to sandy soil with fines content (FC) of less than 20%. Figure 8.13 shows the relationship between fines content (FC) and SPT-N values measured between piles after improvement. An increase of fines content will decrease the increment of the SPT-N value after improvement.

2. Method B (SPT-N and D_r and e relation)

SPT-N and D_r and e relations proposed by Gibbs and Holtz (1957) as shown in Figure 8.14 (b) and (c) and the relationship between grain size and e_{max} and e_{min} shown in Figure 8.14 (a) are used for this method. The D_r and e relation is established from e_{max} and e_{min} assumed from D_{60} of the soil.

The void ratios of original and improved ground e_0 and e_1 are determined from N_0, N_1 and the effective overburden pressure (σ_v') and then the replacement ratio can be found from the following equation:

$$a_s = \Delta e/(1 + e_0) = (e_0 - e_1)/(1 + e_0)$$

The effective overburden pressure (σ_v') is assumed to be equal to the overburden pressure calculated at a depth of 1/2 or 1/3 of the thickness of the improved soil layer.

3. Method C (methods considering fines content)

This method is in principle the same as Method B. A reduction factor (β) defined as shown in the following equation, which will vary in accordance with fines content (FC), is employed in Method B.

$$\beta = \frac{\Delta N}{\Delta N'} = \frac{N_1 - N_0}{N_1' - N_0} = 1.05 - 0.51 \log_{10} FC(\%)$$

Where; N_1': SPT-N value after the improvement with no effect of fines content.

Figure 8.15 shows the relationship between the reduction factor and fines content. β decreases from unity with increase of fines content. The replacement ratio (a_s) calculated in Step-6 in Table 8.1 will be bigger than that for soil without fine particles. Meyerhof's equation and Hirama's experimental formula are used for SPT-N and D_r and e relations for estimation of e_{max} and e_{min}, respectively. Judgement on the possibility of liquefaction during earthquakes fro sandy soils containing fines will have to be made using the liquefaction resistance factor (F_L) obtained from Method C.

(a) Relationship between original N-value N_0 and N-value between piles N_1

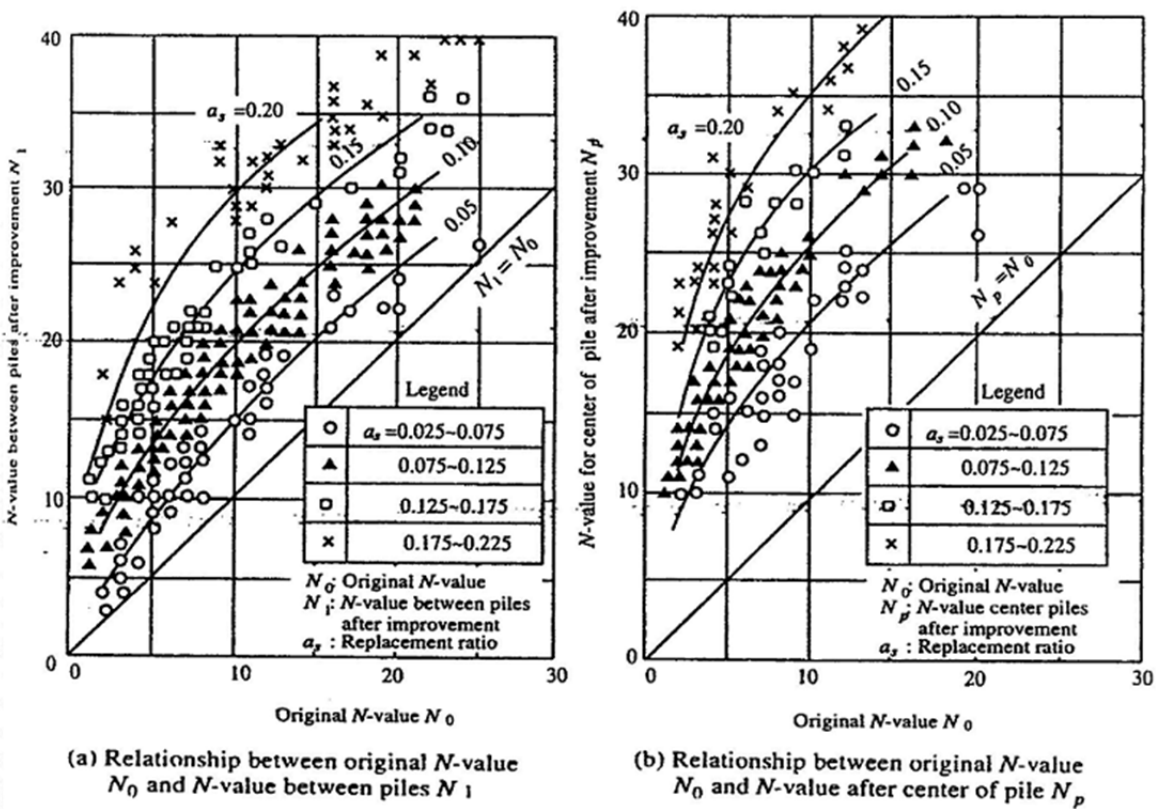(b) Relationship between original N-value N_0 and N-value after center of pile N_p

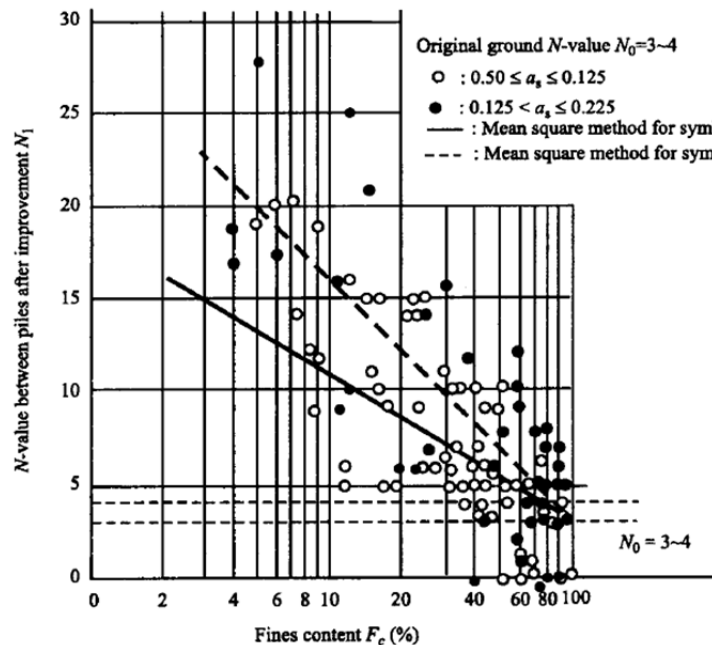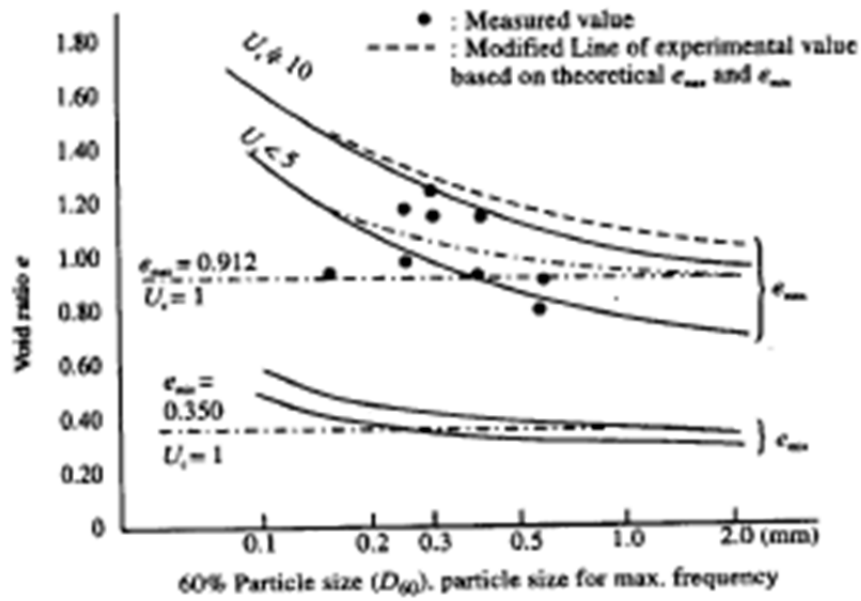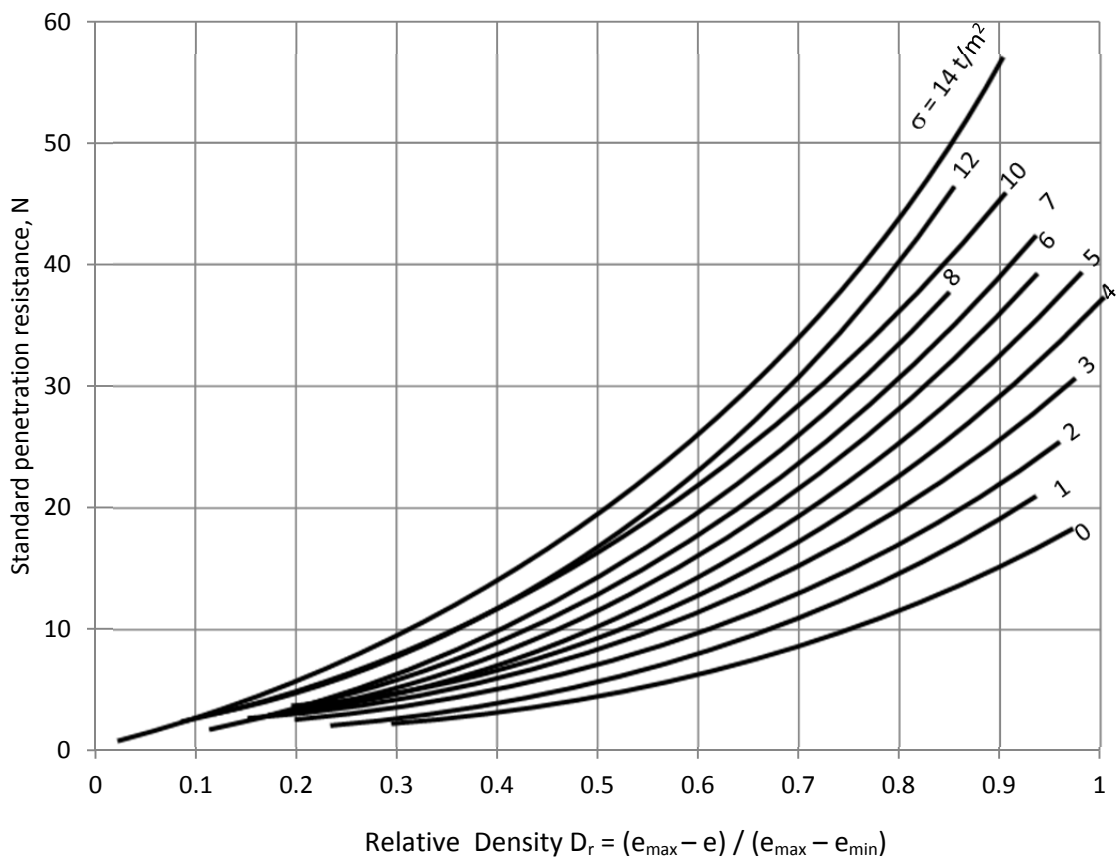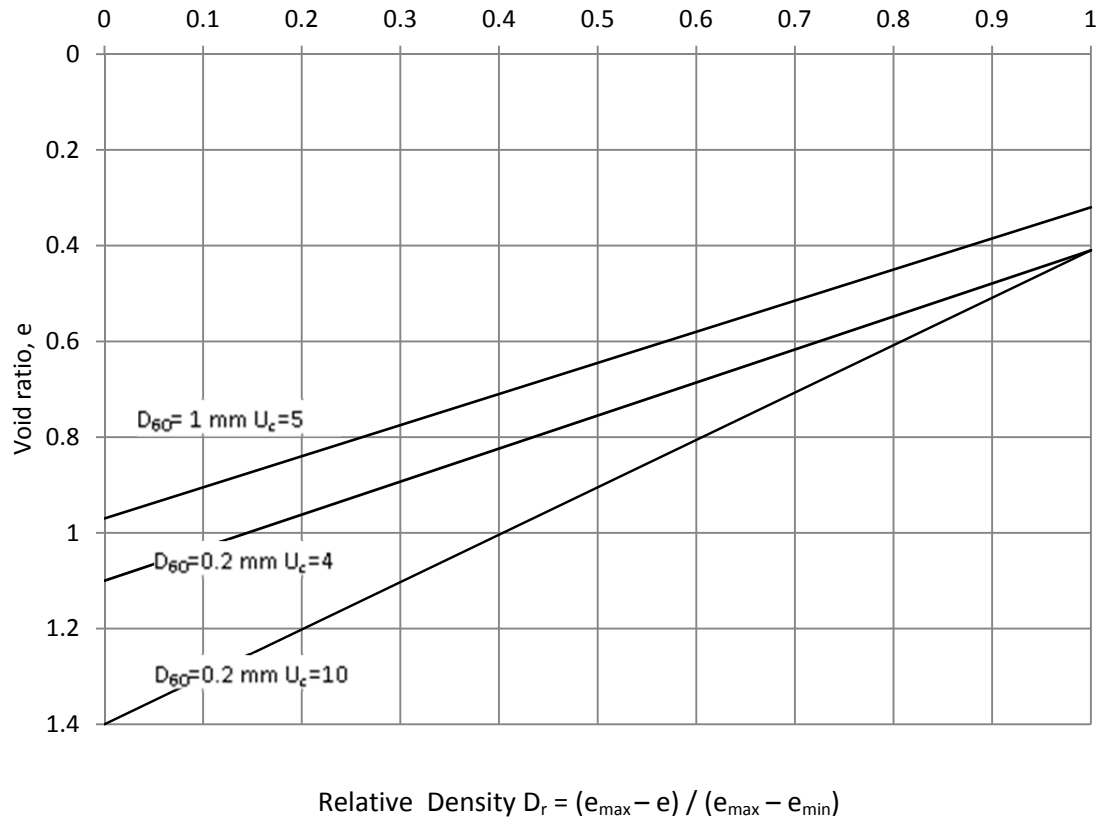**Figure 8.12. Design charts for sand compaction piles (Method A)**

Figure 8.13. Relationship between fines content and SPT-N value after improvement

(a) Relationship between particle size · grain size and e_{max}, e_{min}

Relative Density $D_r = (e_{max} - e) / (e_{max} - e_{min})$

(b)

Relative Density $D_r = (e_{max} - e) / (e_{max} - e_{min})$

(c)

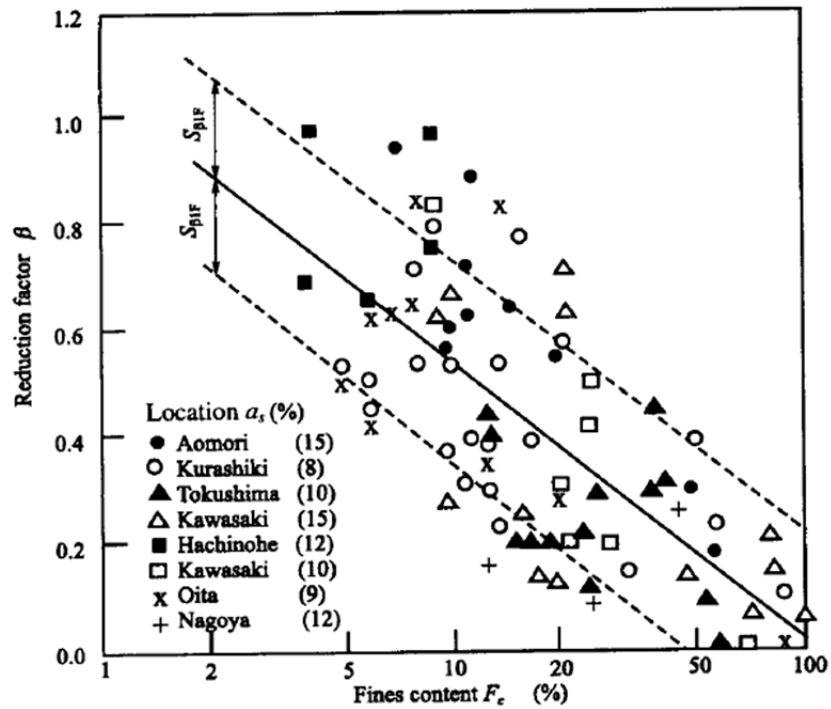**Figure 8.14. Design charts for sand compaction pile (Method B)**

Figure 8.15. Relationship between fines content and reduction factor for improvement of SPT-N value

8.5. Vibro-Replacement Method (Stone Columns)

8.5.1. Application Principles

Empty volume formed by the penetration of vibrator is filled by crushed stone and by the compaction of it rigid columns are performed. In this method, by the provided lateral stresses, surrounding soil is partially consolidated and improved. However this partial improvement is ignored in the design of stone columns. The composite structure, i.e. rigid stone column and soft soil, has s significiantly higher strength and lower compressibility compared with the original soil.

In the stone column applications, under the uniform surface pressure load acting on the single stone column is at an amount of 20 tons to 50 tons. Most efficient improvements are satisfied in soils having undrained shear strength of 15 – 50 kN/m^2. General application depth is within 6 to 10 meters.

8.5.2. Design

Design Principle: Unit Cell Approach

Unit cell approach is the basic theory for stone columns proposed by Priebe, which is also known as Priebe Method. According to Priebe Method, stone columns in a large group can be analyzed through unit cell approach (Kirsch and Kirsch, 2010). Unit cell approach assumes unique diameter of stone columns over an infinitely wide area distributed with unique spacing between them. Stone columns except the ones located at the edge of the group are assumed to show same behavior under loaded area.

In unit cell analyses, a stone column located at center of the tributary area and surrounded by soft soil is considered (Figure 8.16). Moreover, since all the columns in a wide area are simultaneously loaded through rigid raft no lateral deformations and shear forces at the boundary surface of the unit cell is assumed (Kirsch and Kirsch, 2010).

The method proposed by Priebe (Bauman and Bauer, 1974; Priebe, 1988, 1993 and 1995; Mosoley and Priebe, 1993) for estimating reduction in settlement due to ground improvement with stone columns also uses the unit cell model. Furthermore the following idealized conditions are assumed:

- The column is based on a rigid layer
- The column material is incompressible
- The bulk density of column and soil is neglected

Hence, the column cannot fail in end bearing and any settlement of the load area results in a bulging of the column, which remains constant all over its length.

In Figure 8.16; D_e is equivalent diameter of unit cell, D is diameter of stone column, A is area of unit cell, A_c is area of stone column, Q is total applied load on unit cell, σ is total applied stress on unit cell, σ_c is stress carried by stone column and σ_s is stress carried by soil.
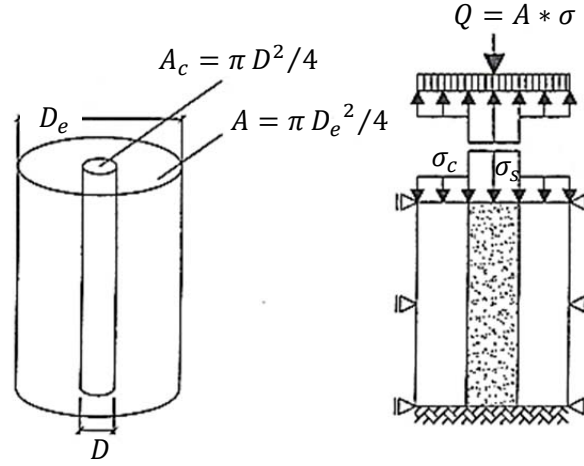
Figure 8.16. Unit cell concept (Kirsch and Kirsch, 2010)

Various group arrangements are illustrated in Figure 8.17 (Madhav, 1982). The equivalent diameter of circular unit cell, D_e, is a function of unique center to center spacing between stone columns, s, i.e.
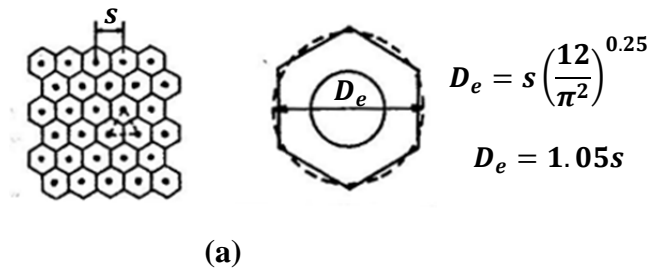
$$D_e = C * s$$

Where the coefficient (C) is,

$$C = \begin{cases} 1.05 & for\ triangular\ pattern \\ 1.13 & for\ square\ pattern \\ 1.29 & for\ hexagonal\ pattern \end{cases}$$

Thus, area replacement ratio (a_r), which is defined as the ratio of area of soft soil replaced by stone column (A_c) to the area of unit cell (A), can be calculated by the following equation:

$$a_r = \frac{A_c}{A} = \frac{1}{C^2}\left(\frac{D}{s}\right)^2$$

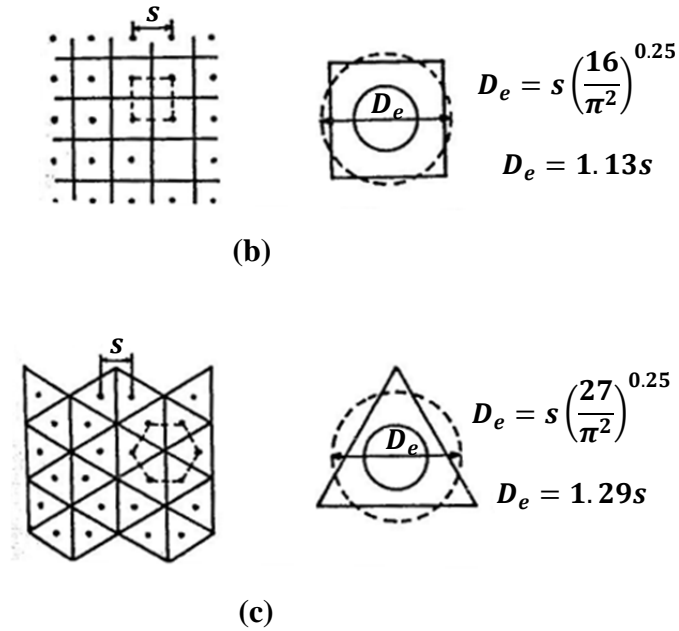$$D_e = s\left(\frac{12}{\pi^2}\right)^{0.25}$$

$$D_e = 1.05s$$

(a)

$$D_e = s\left(\frac{16}{\pi^2}\right)^{0.25}$$

$$D_e = 1.13s$$

(b)

$$D_e = s\left(\frac{27}{\pi^2}\right)^{0.25}$$

$$D_e = 1.29s$$

(c)

Figure 8.17. Different arrangements of stone column groups (a) triangular, (b) square and (c) hexagonal (Madhav, 1982)

Design:

Stress Concentration Factor (n)

Bachus and Barksdale (1989) stated that when a load is applied over soil improved by stone columns, shear strength of stone column increases while settlement in soil decreases. Since the settlement of soil and stone column are approximately same, due to compatibility requirements stress carried by stone columns are larger than the stress acting on soil where the columns are relatively stiffer than soil.

Kirsch and Kirsch (2010) pointed out that the most important parameter controlling the design of stone columns is the stress concentration factor. Stress concentration factor mainly depends on the stiffness of stone column and soil. Since stone column is relatively rigid than the surrounding soft soil, large proportion of applied stress is carried by stone columns. The stress concentration factor (n) is the ratio of stress carried by stone column (σ_c) to stress carried by soft soil (σ_s):

$$n = \frac{\sigma_c}{\sigma_s}$$

By the force equilibrium in vertical direction:

$$\sigma = \sigma_c \frac{A_c}{A} + \sigma_s \left(1 - \frac{A_c}{A}\right) = a_r \sigma_c + (1 - a_r)\sigma_s$$

and,

16

$$\sigma_c = \sigma \frac{n}{[1 + (n-1)a_r]} = \sigma\mu_c \ \ and \ \mu_c = \frac{n}{[1 + (n-1)a_r]}$$

$$\sigma_s = \sigma \frac{1}{[1 + (n-1)a_r]} = \sigma\mu_s \ \ and \ \mu_s = \frac{1}{[1 + (n-1)a_r]}$$

Where; μ_c is the ratio of stress carried by stone column to total applied stress and μ_s is the ratio of stress carried by soil to total applied stress. Stress ratios μ_c and μ_s are related to each other by the following equation:

$$\mu_c = n * \mu_s$$

The elastic finite element study utilizing the unit cell model shows a nearly linear increase in stress concentration in the stone column with increasing modular ratio (Figure 8.18, Barksdale and Bachus, 1983). The approximate linear relation exists for area replacement ratios a_s between 0.1 and 0.25, and length to diameter ratios varying from 4 to 20. For a modular ratio E_s/E_c of 10, a stress concentration factor n of 3 exists. For modular ratios greater than about 10, Barksdale and Bachus (1983) noted that elastic theory underestimates drained settlements due to excessively high stress concentration that theory predicts to occur in the stone and lateral spreading in soft soils. For large stress concentrations essentially all of the stress according to elastic theory is carried by stone column. Since the stone column is relatively stiff, small settlements are calculated using elastic theory when using excessively high stress concentrations.
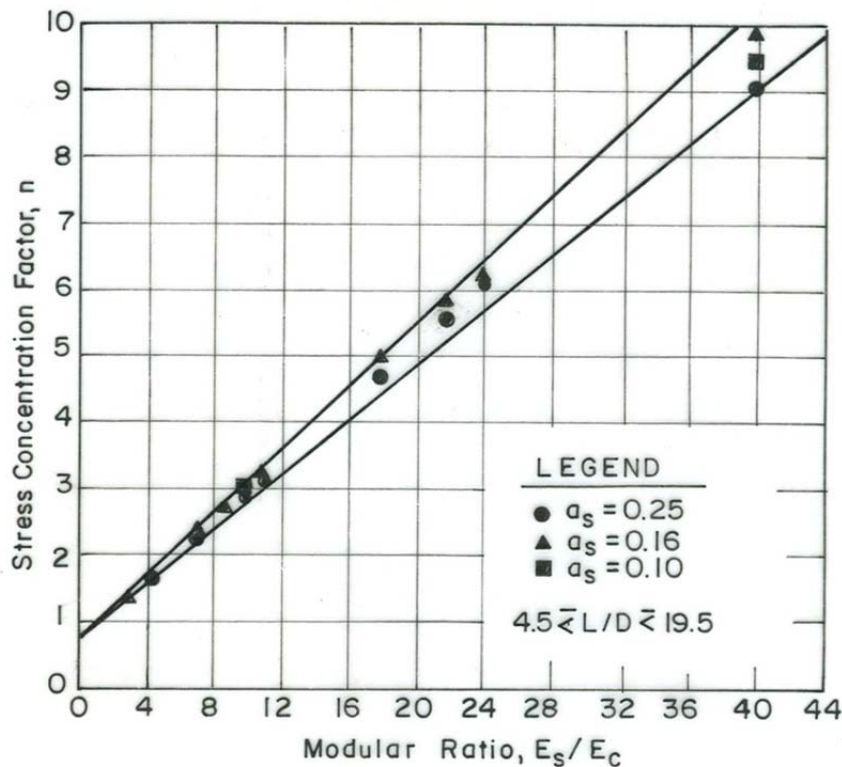
Figure 8.18 Variation of stress concentration factor with modular ratio-linear elastic analysis (Barksdale and Bachus, 1983)

Settlement Improvement Factor (β)

As previously described, unit cell approach assumes equal settlements for stone column and surrounding soft soil, i.e.

$$S_c = S_s$$

Where; S_c: settlement of stone column and S_s: settlement of surrounding soil.

Priebe (1976) is the first researcher who defines settlement improvement factor, β, which is the settlement ratio of untreated soil (S_u) to soil treated by stone columns (S_t). By using the equal settlement assumption, β can be calculated as in the following equation (equilibrium method):

$$\beta = \frac{S_u}{S_t} = \frac{\sigma}{\sigma_s} = 1 + (n-1)a_r$$

Some of the researchers in literature also use the reciprocal of β factor defined as 'settlement reduction ratio'. Settlement reduction ratio is notated by $1/\beta$ or SRR and can be calculated from the following equation:

$$SRR = \frac{1}{\beta} = \frac{S_t}{S_u} = \frac{\sigma_s}{\sigma} = \frac{1}{1 + (n-1)a_r} = \mu_s$$

Based on the compatibility equation ($S_c = S_s$), Priebe (1995) proposed the following expressions for settlement improvement factor, β (Priebe method):

$$\beta = \frac{S_u}{S_t} = 1 + \frac{A_c}{A}\left[\frac{1/2 + f(\nu_s, A_c/A)}{K_{ac}f(\nu_s, A_c/A)} - 1\right]$$

and,

$$f(\nu_s, A_c/A) = \frac{1 - \nu_s^2}{1 - \nu_s - 2\nu_s^2}\cdot\frac{(1 - 2\nu_s)(1 - A_c/A)}{1 - 2\nu_s + A_c/A}$$

and,

$$K_{ac} = \tan^2\left(45° - \frac{\phi_c}{2}\right)$$

Where; ϕ_c: angle of shearing resistance of stone column material and K_{ac}: Rankine's lateral active pressure coefficient for stone column material. Based on the above equations for ν_s=0.3, Figure 8.18 is given by Priebe (1995).
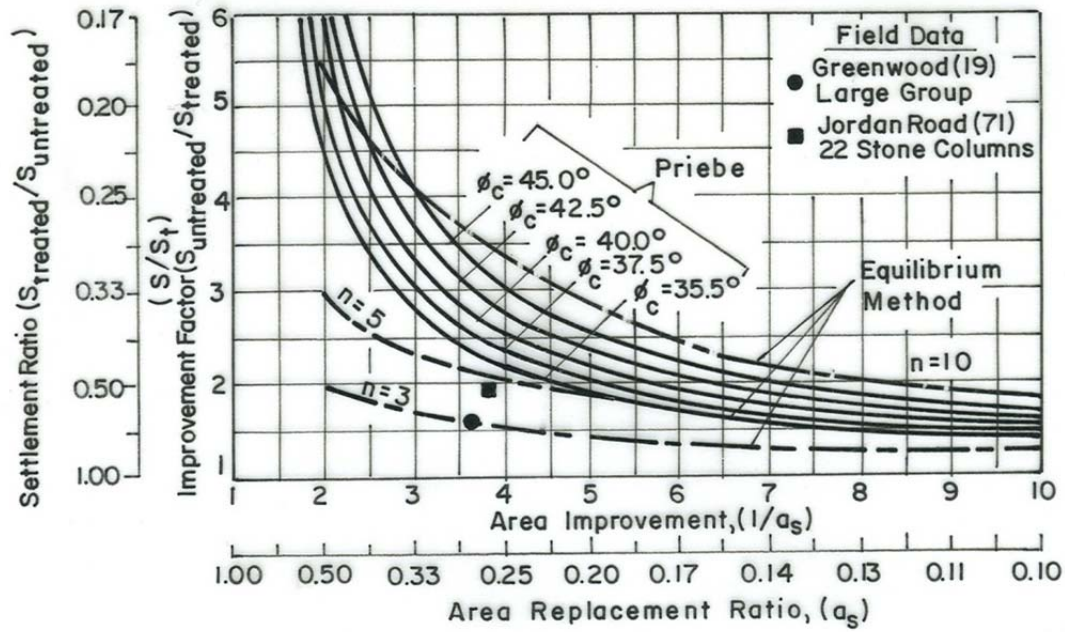
Figure 8.18.Equilibrium and Priebe methods

Load Bearing Capacity of Stone Column (q_{ult})

$$q_{ult} = c_u N_c^*$$

Where;

c_u : undrained shear strength of the clay

N_c^* : bearing capacity factor

Hughes ve Wither (1974) : N_c^* = 25.2 (from model tests)

Thornburn (1975) : N_c^* = 25 (from model tests)

Hughes (1975) :

$$q_{ult} = \tan^2(45° + 0.5\phi') \, (4c_u + \sigma_r')$$
$$q_{all} = q_{ult}/FS$$

Where;

ϕ': internal friction angle of granular material

FS : factor of safety (≈ 1.5 to 2.0)

σ_r' : effective radial stress measured by pressuremeter test (≈ $2c_u$)

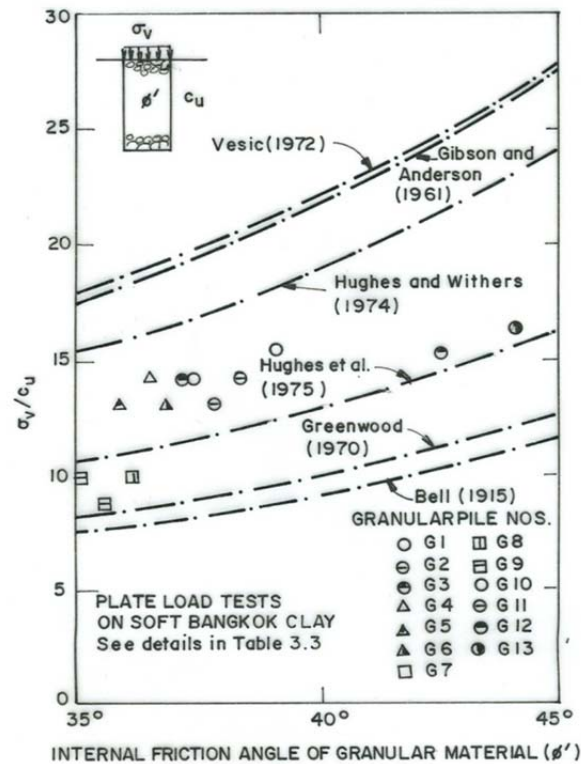Ultimate load bearing capacity of stone columns as proposed by different investigators are given in Figure 8.19.

Figure 8.19. Relationship between internal friction angle of granular material and bearing capacity factor

Relationship between SPT-N values before and after improvement

Relationship between SPT-N values before and after improvement is given in Figure 8.20 for different area replacement ratios.
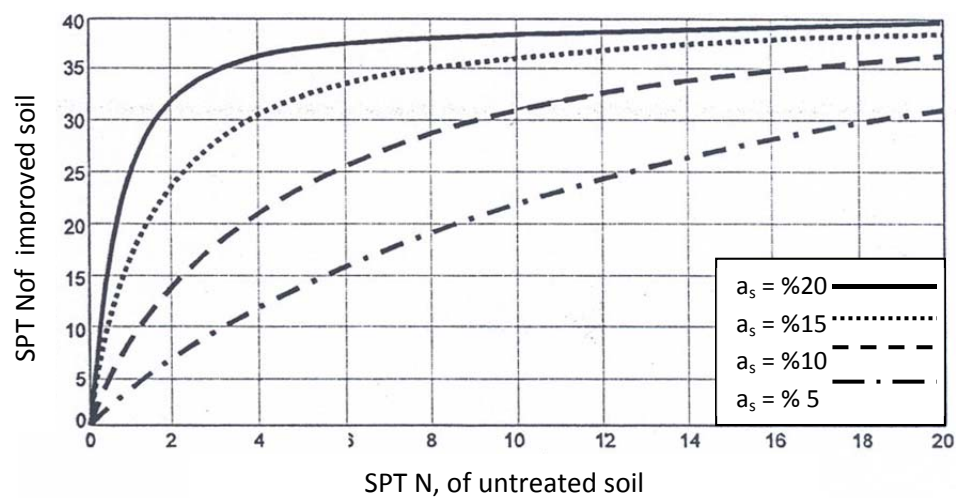

Figure 8.20. Relationship between SPT-N values before and after improvement